IEEE Access
Multidisciplinary ⋮ Rapid Review ⋮ Open Access Journal

Received February 18, 2021, accepted March 30, 2021, date of publication April 5, 2021, date of current version April 14, 2021.

Digital Object Identifier 10.1109/ACCESS.2021.3070798

Nanomaterials Based Nanoplasmonic Accelerators and Light-Sources Driven by Particle-Beams

AAKASH A. SAHAI
Department of Electrical Engineering, College of Engineering, Design and Computing, University of Colorado Denver, Denver, CO 80204, USA
e-mail: aakash.sahai@gmail.com

The work of Aakash A. Sahai was supported by the Department of Electrical Engineering, University of Colorado Denver. This work utilized computational resources of NSF XSEDE RMACC supercomputer that was supported by NSF under Award ACI-1548562, Award ACI-1532235, and Award ACI-1532236.

ABSTRACT Unprecedented tens of TVm^{-1} fields are modeled to be realizable using novel nanoplasmonic surface crunch-in modes in nanomaterials. These relativistic nonlinear surface modes are accessible due to advances in nanofabrication and quasi-solid density sub-micron particle bunch compression. Proof of principle of TVm^{-1} plasmonics is provided using three-dimensional computational and analytical modeling of GeV scale energy gain in sub-millimeter long tubes having nanomaterial walls with controllable free-electron densities, $n_t \sim 10^{22-24}\mathrm{cm}^{-3}$ and hundreds of nanometer core radius driven by quasi-solid electron beams, $n_b \sim 0.01 n_t$. Besides the tens of TeVm^{-1} acceleration gradients, equally strong transverse fields lead to self-focusing and nanomodulation of the beam which drive extreme beam compression to ultra-solid peak densities increasing the crunch-in field strength. Apart from ultra-solid particle beams, extreme focusing also opens up a nano-wiggler like tunable coherent $\mathcal{O}$(100MeV) ultra-dense photon source.

INDEX TERMS Plasmons, crunch-in mode, nanomaterials, electromagnetic propagation, electromagnetic fields, surface waves, nonlinear wave, charge carrier density, particle beams, light sources.

I. INTRODUCTION

Unprecedented TVm^{-1} electromagnetic (EM) fields propounded by Hofstadter [1] in 1968 to be accessible using crystals for ultra-compact particle acceleration have however remained unrealizable. These TVm^{-1} EM fields were also subsequently theorized to be realizable using collective modes [2], [3] in bulk metals driven by charged particle beams. But, the possibility of accessing ultra-strong EM fields in crystals [4], [5] continues to be beset by fundamental obstacles: (i) interaction of a particle beam with ionic lattice of bulk crystals not only results in collisional energy loss and emittance degradation but also drives severely disruptive effects such as filamentation, notwithstanding the favorable effect of channeling of particles along interatomic lattice planes and (ii) the lack of sufficiently intense as well as short bunches required to excite crystal modes.

Tens of TVm^{-1} EM fields of nanometric plasmonic modes (plasmons, surface plasmons, polaritons etc. [6]–[8]) if proven realizable, as endeavored here, would be unparalleled being many orders of magnitude higher than the fields sustained by both the time-tested radio-frequency cavities ($\leq 100\ \mathrm{MeVm}^{-1}$) as well as the upcoming plasma-based ($\leq 100\ \mathrm{GeVm}^{-1}$) techniques [9], [10]. In addition to the immense impact of longitudinal fields for ultra-high gradient particle acceleration, access to tens of TVm^{-1} focusing fields offers unforeseen possibilities such as particle and photon beams of ultra-solid densities.

Furthermore, history of physics is replete with competing advances built on modes in different media: (i) solid-state vs. gaseous lasers; (ii) light emitting diodes (LEDs) vs. compact fluorescent lamps (CFLs) etc. These precedents further motivate the TeraVolts per meter plasmonics as a transformative pathway for extreme EM fields far exceeding the current frontier set by gaseous plasma wakefields [9], [10].

In this work, by unifying advances in nanoscience with the physics of charged particle beams, a novel surface "crunch-in" plasmonic mode [11] shown in Fig.1(a) is uncovered and demonstrated to overcome the fundamental problems of crystals while retaining the key advantages. This relativistic surface plasmonic mode in nanomaterials such as tubes with vacuum-like core not only avoids the direct impact of

The associate editor coordinating the review of this manuscript and approving it for publication was Kin Kee Chow.

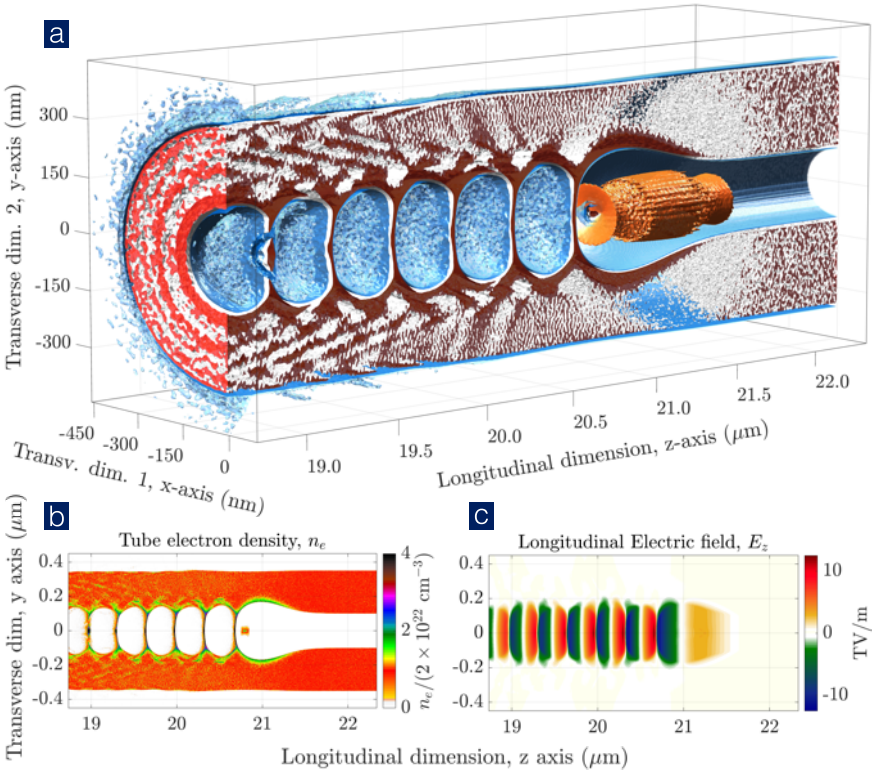

FIGURE 1. 3D PIC simulations showing: (a,b) electron density and (c) longitudinal field profile of tube surface crunch-in mode at around 20μm (around 73fs) of interaction of a $\sigma_z = 400$nm, $\sigma_r = 250$nm beam with nanomaterials in the form of a tube with vacuum-like core radius, $r_t = 100$nm (nearly flat-top limit, $\sigma_r = 2.5 \times r_t$). Here the beam envelope (shown in orange) although initially much larger than the tube has undergone extreme self-focusing approaching ultra-solid densities (see Fig.4 below for details). The tens of TVm^{-1} EM fields in (c) accelerate a subset of the particles of the bunch as demonstrated in Fig.2.

particle beam on bulk ionic-lattice but also utilizes the tunable properties of nanomaterials for optimal excitation of collective oscillations of free electron gas that envelopes the ionic lattice. The nanoplasmonic ''crunch-in'' mode thus opens up access to tens of TVm^{-1} fields.

Earlier work by the author on charged particle beam driven nanoplasmonic [11] ''crunch-in'' mode [12]–[14] in nanomaterials, had modeled a ''sheet'' beam in a two-dimensional (2D) planar geometry. However, in 2D, nonlinear effects such as self-focusing and envelope modulation etc., critical to the underlying crunch-in mechanism are not fully accounted for. Here for the first time three-dimensional (3D) modeling is used to accurately model these effects.

It is further noted that although here the surface crunch-in nanoplasmonic mode is modeled in a single tube, it is in the ''flat-top beam'' limit. In this limit, the beam radial profile is relatively flat compared to the tube core radius. This accounts for the current experimental constraint of beam waist-size (σ_r) being larger than the tube radius (r_t) and a significant portion of the beam interacting with the walls. Therefore, while here the physics is elaborated in a single tube, it is applicable to a wide beam overlapping with an array of tubes.

The novel concept proposed here to access tens of TVm^{-1} EM fields holds promise for the design of future particle colliders as well as non-collider paradigms [15], [16].

II. FRAMEWORK OF THE MODEL

In this section, theoretical framework underlying the proof-of-principle model of the nonlinear surface ''crunch-in'' plasmonic mode [11]–[14] is presented.

A. NANOPLASMONIC MODES IN NANOMATERIALS

The proof-of-principle model relies on the convergence of sub-micron bunch length compression techniques underlying the emergent quasi-solid density particle bunches [17], [18] with the advances in nanofabrication [19]–[23]. Nanofabrication make possible nanoscale structural tunability of nanomaterials, for instance the diameter of vacuum-like core region and thickness of the walls of the tube apart from the characteristics of wall material.

These advances allow quasi-solid density charged particle bunches propagating inside tubes with vacuum-like core [19] of hundreds of nanometer radius, r_t and free-electron gas densities in the nanomaterial wall, $n_t \sim 10^{22-24}$cm^{-3} to drive the wall electrons to collectively crunch deep into its core [12], [13] (shown in Fig.1). Strong electrostatic component of this

crunch-in surface wave based upon collective oscillations of free electron gas thus sustains many TVm^{-1} fields despite the void core and without the direct impact of the bunch on ionic-lattice. This in-vacuum propagation of the most populated part of the bunch overcomes adverse effects such as collision driven energy loss and emittance degradation [4], [5] apart from mitigating severe beam disruption such as filamentation [30] etc. in bulk solids.

Excitation of the surface crunch-in mode in nanomaterials based tubes is also significantly more adaptable compared to bulk modes in unstructured solids [4], [5]. This is because surface modes rely on nanofabrication to better control material composition, density, thickness etc. [19]–[23] to greatly reduce the constraints on the interaction parameter space such as beam properties, alignment etc.

Submicron long charged particle bunches that are now accessible, are here demonstrated to be short enough for controlled excitation of the crunch-in mode. In a quasineutral ideal electron gas of density n_0, effective excitation of wakefields necessitates bunch compression of the order of $\omega_{pe}^{-1}[n_0] = [4\pi n_0 e^2 m_e^{-1}]^{-1/2} = 177(n_0[10^{22}\mathrm{cm}^{-3}])^{-1/2}$ attoseconds and $\lambda_{pe}[n_0] = 2\pi c\omega_{pe}^{-1} = 333(n_0[10^{22}\mathrm{cm}^{-3}])^{-1/2}$ nm [2], [3].

Access to many TVm^{-1} "wavebreaking" fields, $E_{wb}[n_0] = m_e c e^{-1}\omega_{pe}[n_0]$ further requires sufficient energy density which additionally necessitates a minimum number of particles in the ultrashort bunch. Approaching the coherence (wavebreaking) limit of nanoplasmonic fields, $E_{wb} \simeq 9.6(n_t[10^{22}\mathrm{cm}^{-3}])^{1/2}$ TVm^{-1} [24] by strongly exciting the crunch-in mode thus requires quasi-solid density beam, $n_\mathrm{b} \sim 0.01\ n_\mathrm{t}$. Although metallic solids generally have free electron densities in excess of $10^{22}\mathrm{cm}^{-3}$, nanoscale structural engineering offers the possibility of tuning the average or apparent free electron gas density over the spatial scales of plasmonic oscillations.

Detailed physics of the crunch-in mode is elucidated in sec.III using 3D computational (sec.III-A) and analytical (sec.III-B) model. In order to breakdown our analysis to its key principle a single tube of nanomaterial is used. Whereas in a realistic sample there may be a large number of tubes stacked together, the key principle elucidated in a single tube still holds in all the tubes of such a stack. Secondly, as the strength of the crunch-in mode is analytically shown to directly depend upon the beam density relative to the nanoporous wall density (n_b/n_t), an initially large density beam is used to help uncover the key effects in a fewer computational steps (and cost).

B. ATTOSECOND COLLISIONLESS DYNAMICS OF STRONGLY-DRIVEN FERMI ELECTRON GAS

The motion of conduction electrons across a solid surface under the action of static high-fields (known as "field emission") is well known [32], [33]. Being fundamental to this process, tunneling probability is known to increase with the strength of the applied static electric field. Electric fields of ultrashort solid density charged particle beams considered here are of the order of many $100\mathrm{GVm}^{-1}$ while they may only act on the solid surface for femtosecond durations. Therefore, this work utilizes a novel phenomenon of ultrashort tunneling of conduction electrons across a nanoporous surface occurs under the fields of an ultrashort beam. Alternatively, the hundreds of eV potential of solid beams over atomic scales (~ 10Å) is significantly higher than the few eV work function in nanomaterials [34].

Apart from being unbound from the surface, the Fermi electrons gas acquires relativistic momenta over atomic scales in the presence of TVm^{-1} beam fields. In contrast, the known collective or plasmonic modes have oscillatory velocities just higher than the Fermi velocity, v_F [2], [3] which is only around $0.01\ c$.

Furthermore, whereas the collisionless nature of plasmonic oscillations in metals [2], [3] or on its surface [6], [7] is known to have characteristic mean free paths (λ_mfp) of the order of tens of nanometers (despite the sub-nanometer inter atomic spacing) [35]–[37], micron-scale mean free paths, λ_mfp [38] measured in nanomaterials which offer a high degree of control over the size of nano-pores further enhance the collisionless behavior compared to bulk crystals. It is also important to note that the mean free path is, in general, directly proportional to the electron oscillation velocity ($\lambda_\mathrm{mfp} \propto \langle v_e \rangle$) which in our work is relativistic and nearly two orders of magnitude higher than Fermi velocity, v_F. In other words, collision cross-section is, in general, inversely proportional to the particle energy. Therefore, existing estimates of mean free path in solid lattices measured at the v_F are not applicable to relativistic oscillations.

Several unique characteristics thus underlie the novel solid-state collective mode uncovered here. Firstly, it is a relativistic nonlinear generalization of the surface plasmon polariton (SPP) mode [8]. Secondly, while the SPP mode is sustained by small-scale surface electron oscillations, here the oscillation amplitudes can be as large as the tube radius with electrons oscillating deep into the tube core. Lastly, quintessential solid-state properties (non-local) such as energy quantization and ion lattice structure become less relevant because oscillation energies significantly exceed the Fermi energy, $\mathcal{E}_F$. Due to these distinctive characteristics, collective electron dynamics behind the relativistic surface excitation of nanomaterials approximates that of a collisionless quasineutral electron gas in background ionic lattice.

C. TECHNOLOGICAL TRENDS TOWARDS REALIZATION

The thrust towards attosecond particle bunch [17], [18] compression favors effective excitation of nanometric modes. Gaseous plasmas with $n_0 \simeq 10^{16-18}\mathrm{cm}^{-3}$ ($\omega_{pe}^{-1} \simeq \mathcal{O}(10\mathrm{fs})$) have set a precedent on using sub picosecond, micron scale (i) chirped pulse amplified [39] optical lasers and (ii) phase-space gymnastics based compression [17], [18] or plasma based self-modulated particle bunches to make possible the demonstration of GVm^{-1} fields.

Apart from the sub-micron bunch length compression being commissioned at experimental or test facilities such FACET-II [17], [18] near solid submicron bunches are also currently within the reach of x-ray free electron lasers [31] (XFEL) which use a few micron few nC electron bunches that can be modified to obtain the desired dense bunches. Currently accessible beams that approach the desired properties can drive wavebreaking fields ($\sim E_{wb}$) by relying on favorable transverse crunch-in fields which can rapidly self-focus and also self-modulate the beam.

On the other hand, trends of advances in nanofabrication offer the crucial advantage of atomic scale structural design. Investigations of commercial fiber-like tubes [19] (ceramic, polymer, silica or carbon etc.) using a scanning electron microscope reveal a vacuum-like core with a few nm wall-to-core transition. Deposition of nanoporous material using nanofabrication techniques such as atomic layer deposition [20], chemical vapor deposition or similar processes in a hundreds of nanometers thick layer to form the inner tube surface allows controllable apparent free electron density on the inner surface. This density is tunable to significantly below metal-like free electron density using fabrication parameters such as the metal fill-fraction or nano-pore size. For instance, nanoporous (NP) metals such as NP Gold (Au, with bulk free electron density, $5.9 \times 10^{22}\text{cm}^{-3}$) [21], [22] or NP Aluminum (Al bulk conduction or free electron density, $1.8 \times 10^{23}\text{cm}^{-3}$) etc. with controllable characteristics can be deposited on a variety of surfaces.

For mechanical stability, a bundle of thousands of tubes will be used where each tube has an overall width of around a micron (modeled below) resulting in a centimeter-scale wide macroscopic sample (and a train to extend the length). Apart from mechanical stability, such a macroscopic sample containing thousands of tubes in the bundle will allow translation to enable the micron-scale beam spot to be able to interact with a different fresh region of the sample, especially if there is damage. As noted above, the below physics is elucidated in the flat-top beam limit where beam is much wider than the radius of a single tube, thus the same underlying physics of crunch-in regime occurs in multiple tubes.

D. CRUNCH-IN MODE IN CONTRAST WITH PURELY ELECTROMAGNETIC SURFACE MODES

A nanofabricated tube with a vacuum core of tunable hundreds of nanometer radius, r_t and effective wall density, n_t is here introduced to sustain novel crunch-in mode where a significant fraction of the relativistically oscillating tube wall electrons crunches into the core [12]–[14]. It is the crunch-in nonlinear surface wave mode that makes possible the excitation of wall density wavebreaking fields ($E_{wb}[n_t]$) due to its electrostatic nature. However, the surface plasmonic crunch-in mode is yet to be modeled and understood.

It is quite critical to note that here we analytically and computationally model in 3D the surface crunch-in mode, a novel nonlinear surface wave with strong electrostatic field component which is significantly different from conventional and well established "purely" electromagnetic transverse magnetic ($\text{TM}_{\text{m,n}}$, where m,n are the mode numbers) surface modes. In $\text{TM}_{\text{m,n}}$ surface modes the wall electrons are confined to the wall surface and thus the field that is sustained outside the walls inside the cavity, is not electrostatic. Therefore, the distinctive crunch-in mode is not to be confounded with the $\text{TM}_{\text{m,n}}$ surface modes based acceleration mechanism behind dielectric wake acceleration [25], dielectric laser acceleration [26], hollow-channel plasma wakefield regime [27], [28] and rf or beam driven metallic cavities [29].

Experiments using tube-like but partially hollow gaseous plasmas wakefields [40] have reported purely EM modes with relatively weak gradients of $\leq 200\,\text{MVm}^{-1}$ and zero focusing forces. Similarly, gaseous hollow-channels have been used to guide a focussed optical laser for plasma based electron acceleration [41]. However, formation of desired tube-like structures in gaseous plasmas is against its natural tendency and has proven extremely difficult.

Moreover, as it is well established that the purely EM $\text{TM}_{\text{m,n}}$ surface modes sustain zero focusing forces [27], [28] yet highly disruptive transverse fields under symmetry-breaking imperfections. However, due to the strong electrostatic component of the crunch-in mode, previous results on beam dynamics under the action of purely electromagnetic modes are not applicable. Additionally, whereas the purely electromagnetic modes can be modeled using a set of equations based on fluid theory and macroscopic Maxwell equations, the crunch-in mode sustained by nonlinear surface electron oscillations which can have relativistic momentum requires treatment using kinetic theory as elucidated below.

III. PROOF-OF-PRINCIPLE MODEL

A. CRUNCH-IN MODE IN NANOMATERIAL TUBE: 3D COMPUTATIONAL MODEL

Proof of principle of the nanoplasmonic crunch-in mode mechanism in a tube with nanomaterial wall is established using 3D Particle-In-Cell (PIC) simulations. In Fig.1(a,b) the tube surface crunch-in mode driven by a sub-micron long electron beam is evident from the 3D PIC electron density. The ionic lattice is stationary over tens of electron oscillations and the particle density is initialized to be zero within the tube core, $|r| < r_t$. Longitudinal fields in excess of $10\,\text{TVm}^{-1}$ ($10\,\text{TVm}^{-1}$ wall focusing fields, see below) are evident in Fig.1(c) ($E_{wb}[n_t = 2 \times 10^{22}\text{cm}^{-3}] = 13.6\,\text{TVm}^{-1}$).

The 3D simulations in Fig.1 are carried out with EPOCH code [43] which incorporates quantum electrodynamics (QED) effects. A $3.6 \times 1.52 \times 1.52\ \mu\text{m}^3$ cartesian box with 2nm cubic cells is setup. The electrons in the tube of wall density, $n_t = 2 \times 10^{22}\text{cm}^{-3}$ are modeled using 4 particles per cell with fixed ions. The tube has a radius, $r_t = 100\text{nm}$ and wall thickness, $\Delta w = 250\text{nm}$. An electron beam of peak density $n_{b0} = 5 \times 10^{21}\text{cm}^{-3}$; waist-size $\sigma_r = 250\,\text{nm}$ ($\sigma_r = 2.5 \times r_t$) and bunch length $\sigma_z = 400\text{nm}$ is initialized with 1 particle per cell. The box copropagates with this ultrarelativistic beam, $\gamma_b = 10^4$. While the only requirement on beam relativistic factor is $\gamma_b \gg 1$, here it is

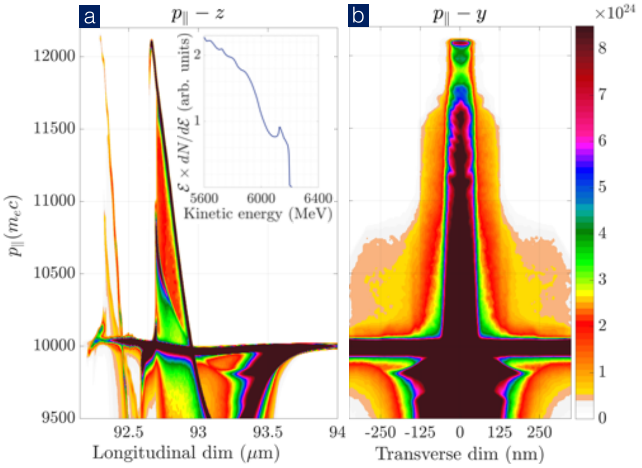

FIGURE 2. 3D PIC simulation beam phase-spaces (a) $p_\parallel - z$ (energy spectrum inset) (b) $p_\parallel - y$ after around 93μm (around 313 fs) of interaction with the tube surface crunch-in mode of Fig.1.

chosen to match with the parameters at the FACET-II facility to motivate experimental verification. Absorbing boundary conditions are used for both fields and particles.

Acceleration of a bunch in the tail of the beam is demonstrated by these 3D simulations. Energy gain of 1.1GeV in 93μm long tube is inferred from the beam longitudinal momentum phase-spaces in Fig.2 along the (a) longitudinal, (b) transverse dimensions. An average acceleration gradient of 11.6 TVm^{-1} is inferred. The accelerated energy spectra inset in (a) is unoptimized because the beam (which is within current reach) used in this proof loads the entire range of acceleration phase.

Note that the beam (initially wider than the tube core) shown in Fig.1(a) has already undergone envelope modulation (in both longitudinally and transversely) under wall focusing forces that are elucidated below in sec.III-C.

B. CRUNCH-IN MODE KINETIC THEORY: 3D ANALYTICAL MODEL

Being highly nonlinear the tube crunch-in mode in Fig.1 is analytically modeled using collisionless 3D kinetic theory. We derive an equation of motion of each individual free electron of nanomaterial wall which experiences the force of charged particle beam. This approach underlies the methodology of a kinetic model [24] unlike the use of moments of the distribution such as density, velocity etc. of a fluid element in fluid theory. These electrons may initially have Fermi-Dirac distribution if in the unperturbed condition they comprised the electron gas of a solid lattice.

A charged particle beam propagates in the z-direction at $c\beta_b$ with a density profile, $n_b(r,z) = n_{b0}\,\mathcal{F}(r,z)$. Initialized with a Gaussian shape

$$\mathcal{F}(r,z) = \exp\left(-\frac{r^2}{2\sigma_r^2}\right)\,\exp\left(-\frac{(z-z_{\max})^2}{2\sigma_z^2}\right),$$

peak density

$$n_{b0} = \frac{N_b}{(2\pi)^{3/2}\sigma_r^2\sigma_z}$$

and

$$N_b = \int_{-\infty}^{\infty}\int_0^{\infty}\int_0^{2\pi} n_b(r,z)\,d\theta\,rdr\,dz$$

particles. The beam is relativistic, $\gamma_b \gg 1$ such that its ''pancake'' electric field is predominantly radial.

A necessary condition for the existence of tube crunch-in mode is the mitigation of ''blowout''. Blowout drives a net momentum flux of all the tube electrons, $\Delta p(r)$ such that they altogether escape the restoring force of the tube ionic lattice. As an extreme case, all the tube electrons within an infinitesimal slice with net charge, $-e\ n_t\ \pi\left[(r_t+\Delta w)^2 - r_t^2\right]\ dz$ may bunch together and pile up into a compression layer just outside the outer tube wall, $r_t + \Delta w$. The net force on this layer is $(F_{\rm beam} + F_{\rm ion})\Delta t = \Delta p$. If the outward force due to the beam, $F_{\rm beam}$ exceeds the restoring force of tube ions, $F_{\rm ion}$ then blowout occurs. The tube and beam parameters thus have to satisfy the crunch-in condition, $\Delta p < 0$,

$$n_t\pi\left[(r_t+\Delta w)^2 - r_t^2\right] > n_{b0}\,\sigma_r^2 \qquad (1)$$

In the above 3D model the ratio of the left over right hand side of eq.1 is greater than 20. It may however be critical to optimize Δw for considerations such as optimal mode spatial profile, vacuum condition etc.

The crunch-in kinetic model defines: r_0 as the equilibrium position of a tube electron with, $r_t < r_0 < r_t + \Delta w$; $r(z,t)$ as the instantaneous radial position of an oscillating free electron; $r_{\rm m}$ as the maximum radius where the driven tube electrons form a compression layer; $\mathcal{H}$ as the step function with $\mathcal{H}(0^+) = 1$ and $\mathcal{H}(0^-) = 0$ to model the effect of step transition in wall density.

The tube electrons which are located at an equilibrium radius less than the electron under consideration at r_0 (between r_0 and r_t) also collectively move with it and compress at the radial extrema, $r_{\rm m}$. When all the tube electrons with an equilibrium radii between r_t and r_0 move together to form a compression layer at a new radial location r, the ionic force on the electron under consideration is $-e\ E_{\rm ion}(r > r_t) = -4\pi e^2\ n_t\ \frac{(r^2-r_t^2)}{2r}$.

In addition to the ionic force, all the electrons with an equilibrium radii smaller than r_0 which collectively move with the electron under consideration result in a collective field opposite to the ionic field. The collective oscillation condition requires that the electrons that originate at an equilibrium position less than r_0 collective move to a position just behind r. The force due to collectively moving tube electrons located between r_0 and r_t is thus $-e\ E_{\rm e}(r) = 4\pi e^2\ n_t\ \frac{(r_0^2-r_t^2)}{2r}$.

The dynamics is different during the radially inward moving phase of the oscillation. Due to the zero ion density in the core region of the tube, the collectively moving electrons do not experience any ionic force inside the core. However, collectively moving tube electrons that originate between r_0 and r_t crunch into the tube core. Inside the core an increase in mutual electrostatic field of the compressing electrons acts to force them back towards equilibrium.

Thus, the net force acting on the electrons is, $F_{\text{collective}} = -m_e \frac{\omega_{pe}^2(n_t)}{2} \frac{1}{r} \left[(r^2 - r_t^2)\,\mathcal{H}(r - r_t) - (r_0^2 - r_t^2)\right]$.

When the tube electrons are driven by an electron (positron, proton) beam with $\text{sgn}[Q_b] = -1$ (+1), they are initially pushed radially outwards (inwards). The acceleration of an oscillating electron as it traverses across the the density discontinuity at the inner surface $r = r_t$ is thus considered, $\frac{d^2 r}{dt^2}|_{r=r_t}\,\mathcal{H}(\text{sgn}[Q_b](r - r_t))$.

The equation of relativistic (γ_e) collective surface electron oscillation is $\gamma_e m_e \frac{\partial^2 r(\xi,z,t)}{\partial t^2} = F_{\text{collective}}$. Equation of the propagating crunch-in surface wave is obtained by transforming to a frame $\xi = c\beta_b t - z$, co-moving with the driver (β_b for an x-ray laser is its group velocity) and using $\partial\xi = (c\beta_b)^{-1}\partial t$. By including the force of the ultrashort drive bunch the crunch-in surface wave equation is,

$$\frac{\partial^2 r}{\partial \xi^2} + \frac{1}{2}\frac{\omega_{pe}^2(n_t)}{\gamma_e c^2 \beta_b^2}\frac{1}{r}\left[(r^2 - r_t^2)\,\mathcal{H}(r - r_t) - (r_0^2 - r_t^2)\right] + \frac{\partial^2 r}{\partial \xi^2}\Big|_{r=r_t}\mathcal{H}(\text{sgn}[Q_b](r - r_t)) = -\text{sgn}[Q_b]\frac{\omega_{pe}^2(n_t)}{\gamma_e c^2 \beta_b^2}\frac{n_{b0}(\xi)}{n_t}\int_0^r dr\,\mathcal{F}(r,z,\xi) \quad (2)$$

With a Gaussian beam envelope,

$$\int_0^r dr\,\mathcal{F}(r,z,\xi) = \frac{\sigma_r^2}{2\pi}\left[1 - \exp\left(-\frac{r^2}{2\sigma_r^2}\right)\right] r^{-1} \times \exp\left(-\frac{(z - z_{\max})^2}{2\sigma_z^2}\right)$$

and under flat-top condition $\sigma_r \gg r_t$, the maxima of the radial trajectory $r = r_m$ is obtained from eq.2. At this maxima, force of the drive beam equals that of the collective charge separation field. The electrons located between r_m and r_t collectively move and bunch together into a compression layer at,

$$r_m = r_t\left(1 - \frac{n_{b0}}{n_t}\frac{2\pi\sigma_r^2}{\pi(r_t + \Delta w)^2}\right)^{-1/2} \quad (3)$$

The net charge of the electron compression layer that collectively crunches from the tube wall into its core can be estimated. During this crunch-in phase the displaced electrons fall into the core region up to a minimum radius, $r_{\min}$. The net charge that falls into the core region is

$$\delta Q_{\max}(r_{\min}) = -e\,n_t\,\pi r_t^2\left(\frac{n_{b0}\,2\pi\sigma_r^2}{n_t\pi(r_t + \Delta w)^2 - n_{b0}\,2\pi\sigma_r^2}\right) dz.$$

The radial electric field is thus obtainable applying the Gauss's law on $\delta Q_{\max}$. Although an analytical expression for $r_{\min}$ can be obtained, we consider $r_{\min} = r_t/\alpha$. The radial electric field is

$$E_{t-r}(r_t) = -\alpha\,n_t\,2\pi r_t\left(\frac{e n_{b0}\,2\pi\sigma_r^2}{n_t\pi(r_t + \Delta w)^2 - n_{b0}\,2\pi\sigma_r^2}\right)$$

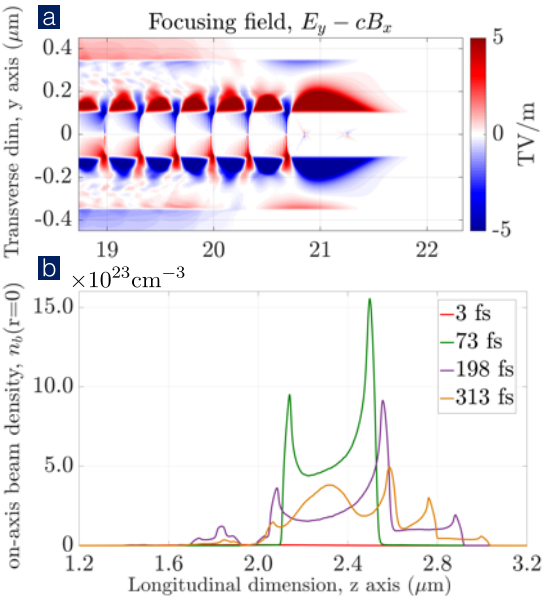

FIGURE 3. 3D PIC simulation with same parameters as in Fig.1: (a) tube crunch-in mode focusing field, (b) time evolution of the on-axis beam density profile which demonstrates extreme beam self-focusing driven nanomodulation of the longitudinal envelope and compression of the transverse envelope resulting in ultra-solid peak densities.

which simplifies to,

$$E_{t-r} = -\alpha\sqrt{\frac{2}{\pi}}\frac{Q_b[\text{pC}]}{\sigma_z[100\text{nm}]}\frac{1}{r_t[100\text{nm}]} \times \left(\left(\frac{r_t + \Delta w}{r_t}\right)^2 - 2\frac{n_{b0}}{n_t}\frac{\sigma_r^2}{r_t^2}\right)^{-1}\frac{\text{TV}}{\text{m}} \quad (4)$$

The peak longitudinal electric field is derived using the Panofsky-Wenzel theorem, $E_{t-r}\,\Delta r = E_{t-z}\,\Delta\xi$ [44]. The value of E_{t-z} varies over $\kappa\sqrt{\gamma_e}\,2\pi c/\omega_{pe}(n_t)$ where κ is the shortened phase of the nonlinearly steepened surface wave, where the tube electrons crunch into its core. The relativistic factor, γ_e ($\simeq (1 + (p_r^2/(m_e c)^2)^{1/2}$) reduces the oscillation frequency as $\omega_{pe}(n_t)/\sqrt{\gamma_e}$. Using $p_r = F_{\text{beam}}\,\sigma_z/c = 4\pi e^2\,n_t c^{-1}\,n_{b0} n_t^{-1}\,r_t\sigma_z(4\pi)^{-1}$, the peak longitudinal field is thus, $E_{t-z} = E_{t-r}\,r_{\min}(\kappa\,2\pi c)^{-1}\,\omega_{pe}(n_t)\gamma_e^{-1/2}$ or,

$$E_{t-z} = -\frac{2}{\kappa}\frac{\sqrt{n_t[10^{22}\text{cm}^{-3}]}}{\sqrt{r_t[100\text{nm}]}}\sqrt{Q_b[\text{pC}]}\frac{\sigma_r}{\sigma_z} \times \left(\left(\frac{r_t + \Delta w}{r_t}\right)^2 - 2\frac{n_{b0}}{n_t}\frac{\sigma_r^2}{r_t^2}\right)^{-1}\frac{\text{TV}}{\text{m}} \quad (5)$$

The expressions of tube crunch-in mode in eq.4 and eq.5 are applicable only if the crunch-in condition in eq.1 is strictly satisfied. Moreover, closer to the critical point in eq.1 the field amplitudes more strongly depend on the ratio.

For $n_t = 2\times 10^{22}\text{cm}^{-3}$, $r_t = 100$nm and $Q_b = 315$ pC, $\sigma_r = 250$nm, $\sigma_z = 400$nm; $r_m = 74.5\text{nm} + r_t$, $E_{t-r} = \alpha\ 8.96$ TV/m (eq.4) and $E_{t-z} = \kappa^{-1}\ 3.5$ TV/m (eq.5) in good agreement with the above 3D simulation.

C. CRUNCH-IN MODE FOCUSING FIELDS: NANOMODULATION AND NANO-WIGGLER EFFECT

The beam envelope in eq.2 is considered to be quasi-stationary over several surface oscillations. Over longer interaction lengths, however, transverse envelope oscillations result in the variation of beam spatial profile, $\mathcal{F}(r, z, \xi)$ and peak density, $n_{b0}(\xi)$. A kinetic equation of the radial dynamics of a beam particle at $r_b(\xi, t)$ under the two forces from beam self-fields and the crunch-in focusing fields (in the region of the bared tube wall ions as well as inside the core) can thus also be obtained in the beam frame.

The tube focusing fields and nanometric transverse beam oscillations from the above 3D simulation are elucidated in Fig.3. The beam particles within $r_m > r_b > r_t$ experience transverse focusing and the beam electrons are forced into the core which results in the folding-in of the ''wings'' of the beam. While transverse focusing occurs rapidly, collisions of particles in the beam wings with ionic lattice will contribute to bremsstrahlung photons although of significantly different energies and characteristics relative to photons from transverse focusing of the beam. The beam develops significant nano-modulation of the longitudinal envelope (analogous to micro-modulation in XFELs) with spatial frequencies corresponding to $\lambda_{\rm osc} \sim \mathcal{O}(100\text{nm})$ as shown in Fig.3(b).

Moreover, extreme focusing under tens of TVm^{-1} focusing fields results in peak on-axis beam density of many ten times the initial density, from initial value of $n_{b0}(\xi = 0) = 5 \times 10^{21}\text{cm}^{-3}$ to ultra-solid densities of $n_{b0}(\xi \simeq 100\mu m) = 10^{24}\text{cm}^{-3}$ (as shown in Fig.3(b)). With this rapid rise in the beam density from being quasi-solid to ultra-solid, the crunch-in field amplitude breaches the wave-breaking limit.

As evidenced by the 3D simulations, the tube focusing fields thus not only guide the beam but also suppress the beam breakup (BBU) instability. This is quite unlike the unfavorable deflecting transverse fields and BBU of linear surface mode based hollow-channel plasma regime [45]. Moreover, due to the guiding nature of focusing fields there is inherent tolerance for angular and spatial misalignments between the beam centroid and the axis of the tubes. Detailed analysis of transverse and longitudinal acceptances as well as the conditions under which BBU may become relevant in the crunch-in mode will be addressed in our future work.

The bright $\mathcal{O}(100\text{MeV})$ high-energy photons ($\text{E}_{\rm ph} = hc\, 2\gamma_b^2/\lambda_{\rm osc}$) produced by nanometric oscillations of ultra-relativistic beam particles in the tens of TVm^{-1} wall focusing fields from a nanometric source size ($\sim r_t$) offers a nano-wiggler light source.

It is important to note the difference between the characteristics of the radiation due to collective motion of charged particles as produced by nanomodulation of the beam in crunch-in focusing fields demonstrated here compared to that produced by uncontrolled disruptive processes such as filamentation or transition radiation (under ionization) etc. It is also critical to note that the radiation generated by collective fields of the crunch-in mode is quite distinct from the well established channeling radiation emitted due to particles oscillating in the ionic force exerted by individual atoms of a solid lattice. Furthermore, self-focusing and nanomodulation of the beam increases the crunch-in fields, a self-reinforcing mechanism which results in nano-wiggler instability.

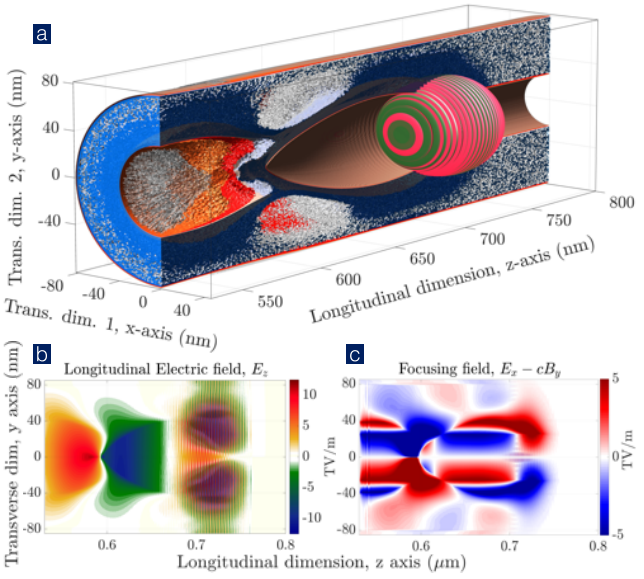

FIGURE 4. 3D PIC simulations of a vaguely similar mode driven in a nanomaterial tube by theoretically proposed nano x-ray laser which ignores the significantly higher level of ionization in a solid lattice due to the high photon energy of such a laser: (a) electron density profile of the wall electrons, (b) acceleration and (c) focusing field profile at around 1μm (3fs) of interaction.

Our future work will investigate schemes to accentuate the collective nature of beam nanomodulation and as a result enhance the properties of the emitted photons using the nano-wiggler instability effect. For instance, variation of tube wall density (nanolattice) or inner radius (corrugated nanomaterials based tube) can further enhance the beam oscillations and allow specific modes to be excited.

Lastly, although a nano x-ray laser is yet to be prototyped, 3D simulation in Fig.4 using a hypothetical 500eV photon energy x-ray laser suggests that it may drive a mode with vague similarities to above. But, this preliminary model is under a very obscure and unjustified assumption that a high photon energy high intensity laser modeled here does not completely ionize the solid lattice (non-plasmonic). In Fig.4, 2.5mJ x-ray pulse is initialized with $a_0 = 2.7$ in line with the conceptual design proposed by Mourou et. al. [42] with $\lambda_0 = 2.5\text{nm}$, pulse length $\tau_{\rm FWHM} = 150$ attosec and waist-size $w_{\rm FWHM} = 25\text{nm}$. The interaction is modeled in a $270 \times 170 \times 170\ \text{nm}^3$ cartesian box with $1.25 \times 1.67 \times 1.67\ \text{Å}^3$ cells. The tube parameters are $n_t = 7.0 \times 10^{22}\text{cm}^{-3}$ (not accounting for ionization), $r_t = 25\text{nm}$ and $\Delta w = 55\text{nm}$. The longitudinal crunch-in field in Fig.4(b) is $E_{t-z} \simeq 12.5\ \text{TVm}^{-1}$ ($E_{wb} = 25.4\ \text{TVm}^{-1}$). The focusing field in Fig.4(c) however differs from Fig.3(a). It is also critical to note that the electron density may dynamically increase due to ionization by the x-ray laser.

IV. CONCLUSION

In conclusion, the 3D computational (PIC) and 3D analytical models demonstrate the realizability of TeraVolts per meter nanoplasmonics. Quasi-solid submicron long multi-GeV electron bunches are demonstrated to effectively excite unprecedented crunch-in nanoplasmonic modes with $\mathcal{O}(\mathrm{TVm}^{-1})$ fields in nanomaterials. We also uncover using 3D modeling that nonlinear surface crunch-in waves sustain many tens of TVm^{-1} focusing fields both in the nanoporous walls and within the core of the tube which result in strong self-focusing. This self-focusing effect increases the peak beam density by orders of magnitude towards ultra-solid densities as well as hundred nanometer scale longitudinal beam density nanomodulation.

Even with currently available electron bunches and nanofabrication technologies, the tube fields can reach unprecedentedly high levels to demonstrate $\mathcal{O}$(GeV) energy gains in sub-mm long nanomaterials. This is possible because the unmatched acceleration gradients, self-focusing and the resulting nanomodulation drive the crunch-in mode more effectively which also opens up controlled coherent $\mathcal{O}$(100MeV) photon production.

Future work will address experimental realization of the proposed nanomaterials based nanoplasmonic accelerator and nanowiggler [46] introduced here using our 3D model. It will also characterize the properties of collective $\mathcal{O}$(100MeV) radiation produced using the nano-wiggler instability and ultra-solid beams for opening new areas of research with a unique combination of high-field, high-energy and high-intensity science. Extreme field frontier accessible using nanomaterials based nanoplasmonic modes elucidated above thus promises to open new pathways in a wide-range of scientific areas.

ACKNOWLEDGMENT

Discussions [47]–[49] at the FACET-II Program Access Committee meeting for the proposal of experiment (Oct 2020), ACN 2020 workshop organized by CERN-ARIES (Mar 2020) and XTALS 2019 workshop at Fermilab (Jun 2019) are acknowledged. The support for this initiative by Profs. T. Katsouleas, G. Mourou, T. Tajima and Dr. Shiltsev is appreciated. The NSF XSEDE RMACC Summit supercomputer utilized here was supported by NSF, the Univ. of Colorado Boulder, and Colorado State Univ. [50], [51].

REFERENCES

[1] R. Hofstadter, "The atomic accelerator," Stanford Univ. HEPL, Stanford, CA, USA, Tech. Rep. 560, 1968.
[2] D. Bohm and D. Pines, "A collective description of electron interactions: III. Coulomb interactions in a degenerate electron gas," *Phys. Rev.*, vol. 92, no. 3, pp. 609–625, Nov. 1953, doi: 10.1103/PhysRev.92.609.
[3] D. Pines, "A collective description of electron interactions: IV. Electron interaction in metals," *Phys. Rev.*, vol. 92, no. 3, pp. 626–636, Nov. 1953, doi: 10.1103/PhysRev.92.626.
[4] P. Chen and R. J. Noble, "A solid state accelerator," in *Proc. Amer. Inst. Phys. Conf.*, vol. 156, 1987, p. 222, doi: 10.1063/1.36458.
[5] P. Chen and R. J. Noble, "Crystal channel collider: Ultra-high energy and luminosity in the next century," in *Proc. AIP Conf.*, vol. 398, 1997, p. 273, doi: 10.1063/1.53055.
[6] R. H. Ritchie, "Plasma losses by fast electrons in thin films," *Phys. Rev.*, vol. 106, no. 5, pp. 874–881, Jun. 1957, doi: 10.1103/PhysRev.106.874.
[7] E. A. Stern and R. A. Ferrell, "Surface plasma oscillations of a degenerate electron gas," *Phys. Rev.*, vol. 120, no. 1, pp. 130–136, Oct. 1960, doi: 10.1103/PhysRev.120.130.
[8] T. K. Sarkar, M. N. Abdallah, M. Salazar-Palma, and W. M. Dyab, "Surface plasmons-polaritons, surface waves, and zenneck waves: Clarification of the terms and a description of the concepts and their evolution," *IEEE Antennas Propag. Mag.*, vol. 59, no. 3, pp. 77–93, Jun. 2017, doi: 10.1109/MAP.2017.2686079.
[9] T. Tajima and J. M. Dawson, "Laser electron accelerator," *Phys. Rev. Lett.*, vol. 43, p. 267, Jul. 1979, doi: 10.1103/PhysRevLett.43.267.
[10] P. Chen, J. M. Dawson, R. W. Huff, and T. Katsouleas, "Acceleration of electrons by the interaction of a bunched electron beam with a plasma," *Phys. Rev. Lett.*, vol. 54, no. 7, pp. 693–696, Feb. 1985, doi: 10.1103/PhysRevLett.54.693.
[11] A. A. Sahai, T. Tajima, P. Taborek, and V. D. Shiltsev, "Solid-state tube wakefield accelerator using surface waves in crystals," *Int. J. Modern Phys. A*, vol. 34, no. 34, Dec. 2019, Art. no. 1943009, doi: 10.1142/S0217751X19430097.
[12] A. A. Sahai, "Excitation of a nonlinear plasma ion wake by intense energy sources with applications to the crunch-in regime," *Phys. Rev. A, Gen. Phys. Beams*, vol. 20, no. 8, Aug. 2017, Art. no. 081004, doi: 10.1103/PhysRevAccelBeams.20.081004.
[13] A. A. Sahai, *On Certain Non-linear and Relativistic Effects in Plasma-based Particle Acceleration*, vol. 8. Durham, NC, USA: Duke Univ., 2015, ch. 8.
[14] A. A. Sahai and T. C. Katsouleas, "Optimal positron-beam excited wakefields in hollow and ion-wake channels," in *Proc. Int. Part. Accel. Conf.*, Richmond, VA, USA, 2015, pp. 2674–2677, doi: 10.18429/JACoW-IPAC2015-WEPJE001.
[15] G. Amelino-Camelia, J. Ellis, N. E. Mavromatos, D. V. Nanopoulos, and S. Sarkar, "Tests of quantum gravity from observations of γ-ray bursts," *Nature*, vol. 393, pp. 763–765, Jun. 1998, doi: 10.1038/31647.
[16] J. Ellis, N. E. Mavromatos, and D. V. Nanopoulos, "Derivation of a vacuum refractive index in a stringy space–time foam model," *Phys. Lett. B*, vol. 665, no. 5, pp. 412–417, Jul. 2008, doi: 10.1016/j.physletb.2008.06.029.
[17] V. Yakimenko, S. Meuren, F. Del Gaudio, C. Baumann, A. Fedotov, F. Fiuza, T. Grismayer, M. J. Hogan, A. Pukhov, L. O. Silva, and G. White, "Prospect of studying nonperturbative QED with beam-beam collisions," *Phys. Rev. Lett.*, vol. 122, no. 19, May 2019, Art. no. 190404, doi: 10.1103/PhysRevLett.122.190404.
[18] V. Yakimenko, "Ultimate beams at FACET-II," in *Proc. Workshop Beam Acc. Cryst. Nanostruct. XTALS*, Jun. 2019, p. 13.
[19] S. Iijima, "Helical microtubules of graphitic carbon," *Nature*, vol. 354, no. 6348, pp. 56–58, Nov. 1991, doi: 10.1038/354056a0.
[20] R. W. Johnson, A. Hultqvist, and S. F. Bent, "A brief review of atomic layer deposition: From fundamentals to applications," *Mater. Today*, vol. 17, pp. 236–246, Jun. 2014, doi: 10.1016/j.mattod.2014.04.026.
[21] J. Erlebacher, M. J. Aziz, A. Karma, N. Dimitrov, and K. Sieradzki, "Evolution of nanoporosity in dealloying," *Nature*, vol. 410, no. 6827, pp. 450–453, Mar. 2001, doi: 10.1038/35068529.
[22] X. Xia, Y. Wang, A. Ruditskiy, and Y. Xia, "Galvanic replacement: A simple and versatile route to hollow nanostructures with tunable and well controlled properties," *Adv. Mater.*, vol. 25, no. 44, pp. 6313–6333, 2013, doi: 10.1002/adma.201302820.
[23] W. Yang, X.-G. Zheng, S.-G. Wang, and H.-J. Jin, "Nanoporous aluminum by galvanic replacement: Dealloying and inward-growth plating," *J. Electrochem. Soc.*, vol. 165, no. 9, pp. C492–C496, 2018, doi: 10.1149/2.0881809jes.
[24] J. M. Dawson, "Nonlinear electron oscillations in a cold plasma," *Phys. Rev.*, vol. 113, p. 383, Jan. 1959, doi: 10.1103/PhysRev.113.383.
[25] W. Gai, P. Schoessow, B. Cole, R. Konecny, J. Norem, J. Rosenzweig, and J. Simpson, "Experimental demonstration of wake-field effects in dielectric structures," *Phys. Rev. Lett.*, vol. 61, no. 24, p. 2756, Dec. 1988, doi: 10.1103/PhysRevLett.61.2756.
[26] R. J. England, R. J. Noble, K. Bane, D. H. Dowell, C. K. Ng, J. E. Spencer, S. Tantawi, Z. Wu, R. L. Byer, E. Peralta, and K. Soong, "Dielectric laser accelerators," *Rev. Mod. Phys.*, vol. 86, p. 1337 Dec. 2014, doi: 10.1103/RevModPhys.86.1337.
[27] T. C. Chiou and T. Katsouleas, "High beam quality and efficiency in plasma-based accelerators," *Phys. Rev. Lett.*, vol. 81, p. 3411, Oct. 1998, doi: 10.1103/PhysRevLett.81.3411.

[28] C. B. Schroeder, D. H. Whittum, and J. S. Wurtele, "Multimode analysis of the hollow plasma channel wakefield accelerator," *Phys. Rev. Lett.*, vol. 82, p. 1177, Feb. 1999, doi: 10.1103/PhysRevLett.82.1177.
[29] S. Y. Kazakov, S. V. Kuzikov, Y. Jiang, and J. L. Hirshfield, "High-gradient two-beam accelerator structure," *Phys. Rev. Special Topics Accel. Beams*, vol. 13, no. 7, Jul. 2010, Art. no. 071303, doi: 10.1103/PhysRevSTAB.13.071303.
[30] A. Benedetti, M. Tamburini, and C. H. Keitel, "Giant collimated gamma-ray flashes," *Nature Photon.*, vol. 12, no. 6, pp. 319–323, Jun. 2018, doi: 10.1038/s41566-018-0139-y.
[31] S. Di Mitri and M. Cornacchia, "Electron beam brightness in linac drivers for free-electron-lasers," *Phys. Rep.*, vol. 539, no. 1, pp. 1–48, Jun. 2014, doi: 10.1016/j.physrep.2014.01.005.
[32] R. H. Fowler and L. Nordheim, "Electron emission in intense electric fields," *Proc. R. Soc. Lond. A, Math. Phys. Sci.*, vol. 119, no. 781, pp. 173–181, May 1928, doi: 10.1098/rspa.1928.0091.
[33] W. Schottky, "Uber kalte und warme Elektronenentladungen," *Zeitschrift für Physik*, vol. 14, pp. 63–106, Dec. 1923, doi: 10.1007/BF01340034.
[34] M. Shiraishi and M. Ata, "Work function of carbon nanotubes," *Carbon*, vol. 39, no. 12, pp. 1913–1917, Oct. 2001, doi: 10.1016/S0008-6223(00)00322-5.
[35] F. Bloch, "Bremsvermogen von Atomen mit mehreren Elektronen," *Zeitschrift für Physik*, vol. 81, nos. 5–6, pp. 363–376, 1933, doi: 10.1007/BF01344553.
[36] S.-I. Tomonaga, "Remarks on Bloch's method of sound waves applied to many-fermion problems," *Prog. Theor. Phys.*, vol. 5, no. 4, pp. 544–569, Jul. 1950, doi: 10.1143/ptp/5.4.544.
[37] E. H. Sondheimer, "The mean free path of electrons in metals," *Adv. Phys.*, vol. 50, no. 6, pp. 499–537, Sep. 2001, doi: 10.1080/00018730110102187.
[38] M. S. Purewal, B. H. Hong, A. Ravi, B. Chandra, J. Hone, and P. Kim, "Scaling of resistance and electron mean free path of single-walled carbon nanotubes," *Phys. Rev. Lett.*, vol. 98, no. 18, May 2007, Art. no. 186808, doi: 10.1103/PhysRevLett.98.186808.
[39] D. Strickland and G. Mourou, "Compression of amplified chirped optical pulses," *Opt. Commun.*, vol. 55, no. 6, pp. 447–449, Oct. 1985, doi: 10.1016/0030-4018(85)90151-8.
[40] S. Gessner, E. Adli, J. M. Allen, W. An, C. I. Clarke, C. E. Clayton, S. Corde, J. P. Delahaye, J. Frederico, S. Z. Green, and C. Hast, "Demonstration of a positron beam-driven hollow channel plasma wakefield accelerator," *Nature Commun.*, vol. 7, no. 1, p. 11785, Sep. 2016, doi: 10.1038/ncomms11785.
[41] A. J. Gonsalves, K. Nakamura, J. Daniels, C. Benedetti, C. Pieronek, T. C. H. De Raadt, S. Steinke, J. H. Bin, S. S. Bulanov, J. Van Tilborg, and C. G. R. Geddes, "Petawatt laser guiding and electron beam acceleration to 8 GeV in a laser-heated capillary discharge waveguide," *Phys. Rev. Lett.*, vol. 122, no. 8, Feb. 2019, Art. no. 084801, doi: 10.1103/PhysRevLett.122.084801.
[42] G. Mourou, S. Mironov, E. Khazanov, and A. Sergeev, "Single cycle thin film compressor opening the door to Zeptosecond-Exawatt physics," *Eur. Phys. J. Special Topics*, vol. 223, no. 6, pp. 1181–1188, May 2014, doi: 10.1140/epjst/e2014-02171-5.
[43] T. D. Arber, K. Bennett, C. S. Brady, A. Lawrence-Douglas, M. G. Ramsay, N. J. Sircombe, P. Gillies, R. G. Evans, H. Schmitz, A. R. Bell, and C. P. Ridgers, "Contemporary particle-in-cell approach to laser-plasma modelling," *Plasma Phys. Controlled Fusion*, vol. 57, no. 11, Nov. 2015, Art. no. 113001, doi: 10.1088/0741-3335/57/11/113001.
[44] W. K. H. Panofsky and W. A. Wenzel, "Some considerations concerning the transverse deflection of charged particles in radio-frequency fields," *Rev. Sci. Instrum.*, vol. 27, no. 11, p. 967, Nov. 1956, doi: 10.1063/1.1715427.
[45] C. A. Lindstrøm, E. Adli, J. M. Allen, W. An, C. Beekman, C. I. Clarke, C. E. Clayton, S. Corde, A. Doche, J. Frederico, and S. J. Gessner, "Measurement of transverse wakefields induced by a misaligned positron bunch in a hollow channel plasma accelerator," *Phys. Rev. Lett.*, vol. 120, no. 12, Mar. 2018, Art. no. 124802, doi: 10.1103/PhysRevLett.120.124802.
[46] A. Sahai, M. Golkowski, F. Zimmermann, J. Resta-Lopez, T. Tajima, and V. Shiltsev, "Nanostructure accelerators: Novel concept and path to its realization," 2020, *arXiv:2006.10261*. [Online]. Available: https://arxiv.org/abs/2006.10261
[47] A. Sahai, "Nano^{2}WA experimental proposal," in *Proc. FACET-II PAC Meeting*, Stanford, CA, USA, Oct. 2020. [Online]. Available: https://facet.slac.stanford.edu/sites/facet.slac.stanford.edu/files/FACETII_PAC_committee_answers_nano2WA_proposal_Sahai.pdf
[48] A. Sahai, "TV/m atomic-scale crunch-in wakefields," in *Proc. Appl. Cryst. Nanotubes Acceleration Manipulation*. Lausanne, Switzerland: CERN ACN, Mar. 2020. [Online]. Available: https://indico.cern.ch/event/867535/contributions/3716404/
[49] A. Sahai, "Nonlinear surface charge-density waves in hollow-channels for wakefield acceleration," in *Proc. Workshop Beam Acceleration Cryst. Nanostruct.* Fermilab, IL, USA: XTALS, 2019. [Online]. Available: https://indico.fnal.gov/event/19478/contributions/52561/
[50] J. Towns, T. Cockerill, M. Dahan, I. Foster, K. Gaither, A. Grimshaw, V. Hazlewood, S. Lathrop, D. Lifka, G. D. Peterson, R. Roskies, J. R. Scott, and N. Wilkins-Diehr, "XSEDE: Accelerating scientific discovery," *Comput. Sci. Eng.*, vol. 16, no. 5, pp. 62–74, Sep. 2014, doi: 10.1109/MCSE.2014.80.
[51] J. Anderson, P. J. Burns, D. Milroy, P. Ruprecht, T. Hauser, and H. J. Siegel, "Deploying RMACC summit: An HPC resource for the rocky mountain region," in *Proc. PEARC*, New Orleans, LA, USA, Jul. 2017, pp. 1–7, doi: 10.1145/3093338.3093379.

AAKASH A. SAHAI received the M.S. degree in electrical engineering from Stanford University, in 2005, the M.S. degree in accelerator physics from Indiana University Bloomington, IN, USA, and the U.S. Particle Accelerator School (USPAS), Fermilab, USA, in 2015, and the Ph.D. degree from Duke University, Durham, NC, USA, in 2015.

Prior to starting his research initiative at CU Denver, from 2015 to 2018, he led several research proposals in the areas of plasma and accelerator physics with the Physics Department, Imperial College London. He currently leads an effort on prototyping of his initiative on TeraVolts per meter nanoplasmonics using nanomaterials with the University of Colorado Denver, Denver, CO, USA. This effort on extreme field physics has wide-ranging applicability cutting across novel accelerators, light-sources to affordable fusion energy alternatives, and so on. His research also focuses on innovations in tunable positron and muon sources using laser-driven plasmas as well as space and astro plasma physics.